Monthly Notices of the ROYAL ASTRONOMICAL SOCIETY

MNRAS **461,** 760–765 (2016) doi:10.1093/mnras/stw1555
Advance Access publication 2016 June 6

Detection of solar-like oscillations in relics of the Milky Way: asteroseismology of K giants in M4 using data from the NASA K2 mission

A. Miglio,[1,2]★ W. J. Chaplin,[1,2] K. Brogaard,[2] M. N. Lund,[1,2] B. Mosser,[3] G. R. Davies,[1,2] R. Handberg,[2] A. P. Milone,[4] A. F. Marino,[4] D. Bossini,[1,2] Y. P. Elsworth,[1,2] F. Grundahl,[2] T. Arentoft,[2] L. R. Bedin,[5] T. L. Campante,[1,2] J. Jessen-Hansen,[2] C. D. Jones,[1,2] J. S. Kuszlewicz,[1,2] L. Malavolta,[5,6] V. Nascimbeni[5] and E. L. Sandquist[7]

[1]*School of Physics and Astronomy, University of Birmingham, Edgbaston, Birmingham B15 2TT, UK*
[2]*Stellar Astrophysics Centre, Department of Physics and Astronomy, Aarhus University, DK-8000 Aarhus C, Denmark*
[3]*LESIA, Observatoire de Paris, PSL Research University, CNRS, Université Pierre et Marie Curie, Université Paris Diderot, F-92195 Meudon, France*
[4]*Research School of Astronomy and Astrophysics, Australian National University, Mt Stromlo Observatory, ACT 2611, Australia*
[5]*INAF – Osservatorio Astronomico di Padova, vicolo dell'Osservatorio 5, I-35122 Padova, Italy*
[6]*Dipartimento di Fisica e Astronomia 'Galileo Galilei', Universitá di Padova, vicolo dell'Osservatorio 3, I-35122 Padova, Italy*
[7]*Department of Astronomy, San Diego State University, San Diego, CA 92182, USA*

Accepted 2016 May 13. Received 2016 May 13; in original form 2015 November 18

ABSTRACT

Asteroseismic constraints on K giants make it possible to infer radii, masses and ages of tens of thousands of field stars. Tests against independent estimates of these properties are however scarce, especially in the metal-poor regime. Here, we report the detection of solar-like oscillations in eight stars belonging to the red-giant branch (RGB) and red-horizontal branch (RHB) of the globular cluster M4. The detections were made in photometric observations from the K2 Mission during its Campaign 2. Making use of independent constraints on the distance, we estimate masses of the eight stars by utilizing different combinations of seismic and non-seismic inputs. When introducing a correction to the $\Delta\nu$ scaling relation as suggested by stellar models, for RGB stars we find excellent agreement with the expected masses from isochrone fitting, and with a distance modulus derived using independent methods. The offset with respect to independent masses is lower, or comparable with, the uncertainties on the average RGB mass (4–10 per cent, depending on the combination of constraints used). Our results lend confidence to asteroseismic masses in the metal-poor regime. We note that a larger sample will be needed to allow more stringent tests to be made of systematic uncertainties in all the observables (both seismic and non-seismic), and to explore the properties of RHB stars, and of different populations in the cluster.

Key words: stars: low-mass – stars: oscillations – globular clusters: individual: NGC 6121 (M4).

1 INTRODUCTION

Asteroseismology has revolutionized our view of evolved stars. The NASA *Kepler* (Koch et al. 2010) and CNES-led *CoRoT* (Baglin et al. 2006) missions have delivered exquisite asteroseismic data that have allowed radii and masses to be estimated for more than 10 000 individual field red-giant stars in the Milky Way. These new results have direct implications for our ability to determine distances and, crucially, to estimate ages of such stars, which are key ingredients for in-depth studies of how the Galaxy formed and evolved.

The strong correlation between mass and age in low-mass red-giant stars means that the required goal of determining stellar ages to 30 per cent or better implies that masses must be estimated to an accuracy better than 10 per cent. Comparisons against accurate and independent mass determinations are however limited to stars in binary systems and, most notably, stars in clusters (see e.g. Brogaard et al. 2015, for a review). Unfortunately, the open clusters observed by the *Kepler* space telescope (during its nominal mission) and by

★ E-mail: miglioa@bison.ph.bham.ac.uk

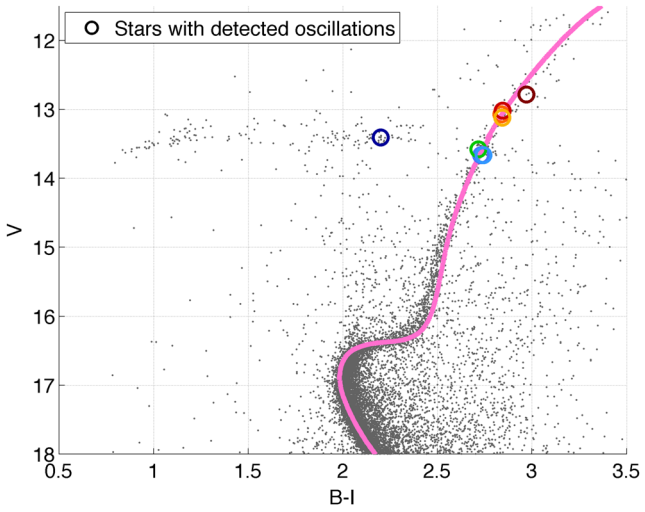

Figure 1. Colour–magnitude diagram (CMD) of M4 stars based on the data set described in D'Antona et al. (2009). Magnitudes and colour were corrected for differential reddening following Milone et al. (2012). The solid line represents an isochrone (from BaSTI, see Section 3.1.1 for details) fit to the CMD. The large coloured open circles mark the stars with detected solar-like oscillations (the corresponding oscillation spectra are plotted in Fig. 2).

CoRoT explored the metal-rich regime only, and did not provide a test of the metal-poor population.

Globular clusters are the oldest stellar systems for which it is possible to make reliable age estimates, and are hence benchmarks to test other age determinations. Previous efforts to detect solar-like oscillations in globular clusters have been made, but either no oscillations were detected (Frandsen et al. 2007), or only marginal detections were made (Stello & Gilliland 2009). However, K2 – the re-purposed *Kepler* mission (Howell et al. 2014) – has now begun a survey of the ecliptic plane, which contains bright clusters including the globular cluster M4. In this Paper, we report the detection of solar-like oscillations in K2 data of K giants belonging to M4, and compare the measured global oscillation properties against those expected from well-constrained, independent distance and mass estimates.

2 M4 DATA REDUCTION AND ANALYSIS

M4 was observed in K2 Campaign 2 for a total of 78.8 d. A fraction of the cluster's total angular area on the celestial sphere was covered by 16 50-by-50 pixel superstamps. Masks for individual targets within the superstamps were defined using the K2P^2 (K2-Pixel-Photometry; Lund et al. 2015) pipeline. Each mask was constructed from a summed image (over time) that allowed for the apparent motion of the stars on the CCD due to the drift of the spacecraft (Howell et al. 2014). Time-dependent positions of stars on the CCD were estimated from the 2D cross-correlation of a given superstamp, instead of estimated centroids for individual targets. A set of unsupervised machine learning techniques was then applied to define the final masks, from which light curves were then produced.

Changes in measured flux due to spacecraft roll were corrected by utilizing the strong correlation of those changes with the stellar position on the CCD, using procedures similar to those described in Vanderburg & Johnson (2014). The resulting, corrected light curves were then cleaned for artefacts using the KASOC filter (Handberg & Lund 2014); time-scales of $\tau_{\rm long} = 1$ d and $\tau_{\rm short} = 0.25$ d were

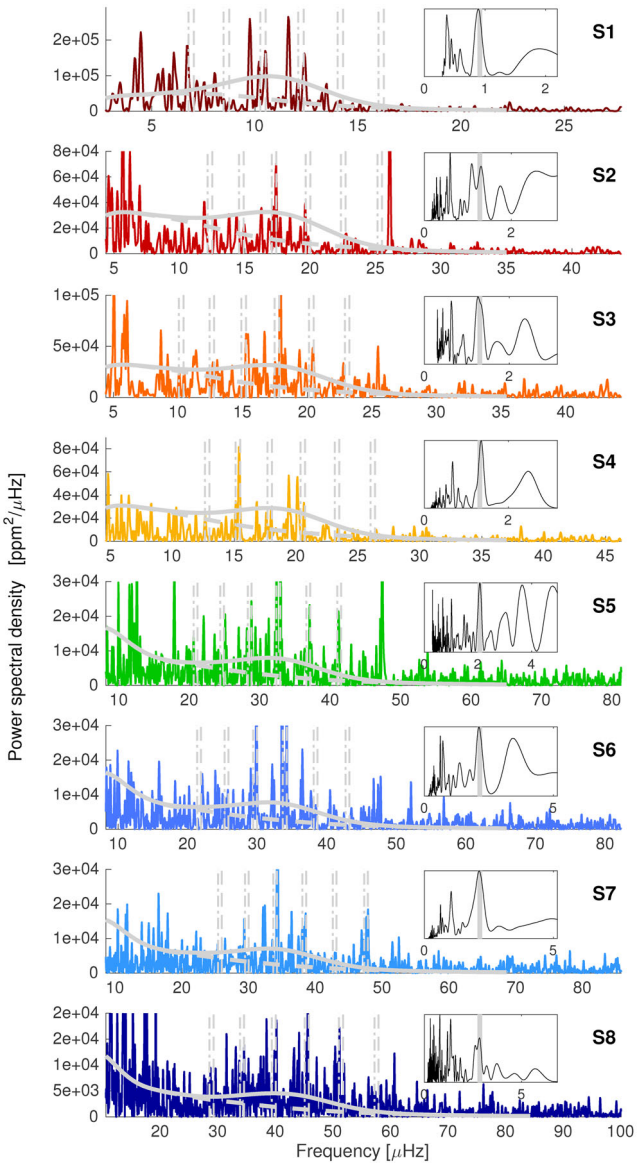

Figure 2. Solar-like oscillation spectra of eight K giants observed by K2. The bottom star is in the RHB. Stars (from top to bottom) are ordered by increasing $\nu_{\rm max}$. Vertical lines show the position of radial (dashed lines) and quadrupole (dash–dotted lines) oscillation frequencies as expected by the pattern of oscillation modes in red-giant stars described in Mosser et al. (2011). The expected granulation power and the combined granulation and oscillation power are represented by dashed and solid thick lines. The insets show the power spectrum of the power spectrum (PSPS) of each star, computed from the region around $\nu_{\rm max}$. In each PSPS, the prominent peak at $\Delta\nu/2$ (vertical grey line) is the detected signature of the near-regular spacing of oscillation peaks in the frequency spectrum.

adopted for the median filters. We refer to Handberg & Lund (2014) for additional details on the KASOC filter.

Among the sources identified by the K2P^2 pipeline, we selected those that could be unambiguously identified as K giants from the D'Antona et al. (2009) catalogue and the Marino et al. (2008, 2011) membership studies. Moreover, we retained only stars with $V < 14$ and $B - I > 1.7$, i.e. we avoided RR Lyrae pulsators, blue-horizontal-branch stars, and stars that would be too faint to have detectable oscillations (see Fig. 1).

We then searched the frequency-power spectra of the chosen set of 28 light curves for evidence of solar-like oscillations using two independent detection pipelines. The first one is based on an updated version (Elsworth et al., in preparation) of the automated detection pipeline described in Hekker et al. (2010, see also Chaplin et al. 2015). The asteroseismic analysis code was then used to extract from the detected oscillation spectra estimates of two commonly used global or average asteroseismic parameters: $\Delta\nu$, the average frequency separation between consecutive overtones of modes having the same angular degree; and $\nu_{\rm max}$, the frequency at which the oscillations present their strongest observed amplitudes (see Elsworth et al., in preparation for details). To compare the detected power with expectations, we used the relations in Mosser et al. (2012) and Kallinger et al. (2014) to describe the power envelope due to the oscillations and the power spectrum of the granulation, to which we then added the contribution due to shot noise estimated from the mean power close to the Nyquist frequency (see Fig. 2). The observed power excess is compatible with expectations, in some cases weaker than expected, but this is in line with the fact that light curves of cluster stars suffer from a higher level of contamination from nearby sources.

We have then performed a second analysis using an independent method that effectively utilizes the expected frequency pattern of red-giant oscillation modes (Mosser et al. 2011). Estimates of the large spacing were first provided by the autocorrelation function (Mosser & Appourchaux 2009), with the requirement that the null hypothesis be rejected at the 95 per cent confidence level. These values were then refined with the method of Mosser et al. (2011). This uses a priori knowledge of the radial and quadrupole frequency patterns and provides reasonable constraints on the spacings even if the spectrum is of moderate quality only (see Fig. 2 and Hekker et al. 2012). Dipole modes, on the other hand, are not used since their frequencies are expected to show a complex pattern originating from the interaction between acoustic and gravity modes. In all cases, we also tested whether the excess power associated with a possible detection of the oscillations was consistent with expectations based on results from archival *Kepler* data. For noisy spectra, the frequency of maximum oscillation was determined as for semiregular variables showing only a limited number of modes (Mosser et al. 2013).

Having compared results, we retained only stars where both pipelines reported a detection of solar-like oscillations (eight stars, labelled S1 to S8; see Table 1 and Fig. 1). Their power spectra are shown in Fig. 2. Seven of the stars (S1 to S7) are on the red-giant branch (RGB); the eighth (S8, spectrum shown in bottom panel) is on the red-horizontal branch (RHB). We adopted values and uncertainties for $\Delta\nu$ and $\nu_{\rm max}$ from the pipeline by Mosser et al. (2011), which are compatible within 1σ with those obtained with the first pipeline. For two stars (S2 and S6), the first pipeline returned two possible solutions for $\Delta\nu$, while results from the Mosser et al. (2011) method returned only a single value (which was compatible with one of the two solutions of the first pipeline).

Given the low fraction of stars in which we were able to unambiguously detect solar-like oscillations, we assessed the noise properties of the light curves analysed, and compared them with those of field stars. The stars analysed in this work have a noise level (calculated as in Stello et al. 2015 as the median power between 260 and 280 μHz) of the order of few hundreds ppm^2 μHz^{-1} (see Table 1), which is a factor ∼5–7 higher than in field stars of similar magnitude as presented in Stello et al. (2015). A thorough assessment of whether the augmented noise is primarily due to the contamination from nearby sources in such a crowded field remains to be addressed. Moreover, tests need to be carried out on how oscillation detection pipelines perform with K2 data sets, which are shorter, and have higher noise (e.g. the instrumental noise peak at $\nu \simeq 47.23$ μHz, see Lund et al. 2015), compared to those provided by the nominal *Kepler* mission.

3 RESULTS AND COMPARISON WITH INDEPENDENT CONSTRAINTS

3.1 Masses

We proceeded as in Miglio et al. (2012) and estimated stellar masses by using several combinations of the available seismic and non-seismic constraints.

The average separation scales to very good approximation as the square root of the mean density of the star, i.e. $\Delta\nu \propto \rho^{1/2}$; whilst $\nu_{\rm max}$ has been found to scale with a combination of surface gravity and effective temperature that also describes the dependence of the cut-off frequency for acoustic waves in an isothermal atmosphere, i.e. $\nu_{\rm max} \propto g T_{\rm eff}^{-1/2}$ (see Chaplin & Miglio 2013 for further details and references).

Four sets of masses were computed, using:

$$\frac{M}{\mathrm{M}_\odot} \simeq \left(\frac{\nu_{\rm max}}{\nu_{\rm max,\odot}}\right)^3 \left(\frac{\Delta\nu}{\Delta\nu_\odot}\right)^{-4} \left(\frac{T_{\rm eff}}{\mathrm{T}_{\rm eff,\odot}}\right)^{3/2}, \quad (1)$$

$$\frac{M}{\mathrm{M}_\odot} \simeq \left(\frac{\Delta\nu}{\Delta\nu_\odot}\right)^2 \left(\frac{L}{\mathrm{L}_\odot}\right)^{3/2} \left(\frac{T_{\rm eff}}{\mathrm{T}_{\rm eff,\odot}}\right)^{-6}, \quad (2)$$

$$\frac{M}{\mathrm{M}_\odot} \simeq \left(\frac{\nu_{\rm max}}{\nu_{\rm max,\odot}}\right) \left(\frac{L}{\mathrm{L}_\odot}\right) \left(\frac{T_{\rm eff}}{\mathrm{T}_{\rm eff,\odot}}\right)^{-7/2}, \quad (3)$$

$$\frac{M}{\mathrm{M}_\odot} \simeq \left(\frac{\nu_{\rm max}}{\nu_{\rm max,\odot}}\right)^{12/5} \left(\frac{\Delta\nu}{\Delta\nu_\odot}\right)^{-14/5} \left(\frac{L}{\mathrm{L}_\odot}\right)^{3/10}. \quad (4)$$

The solar reference values were taken as $\Delta\nu_\odot = 135.1$ μHz, $\nu_{\rm max,\odot} = 3090$ μHz (Huber et al. 2013) and $\mathrm{T}_{\rm eff,\odot} = 5777$ K. The solar reference values for both pipelines used in this work differ from the values quoted by less than 0.5 per cent, hence the size of systematic shifts in mass when using equations (1)–(4) are expected to be lower than the uncertainties on the average RGB mass.

The above equations assume strict adherence to the classic asteroseismic scaling relations for $\Delta\nu$ and $\nu_{\rm max}$.

Photometric $T_{\rm eff}$ were calculated using $(B - V)_0$ and compared with the value obtained using $(V - I)_0$ to check for consistency. We used $E(B - V)$ and $E(V - I)$ values from table 3 in Hendricks et al. (2012). Colour–$T_{\rm eff}$ calibrations, as well as bolometric correction (BC) at the stellar temperatures, and the solar BC were taken from Casagrande & VandenBerg (2014). We iterated between the asteroseismic surface gravity, obtained from $\nu_{\rm max}$ and $T_{\rm eff}$, and the colour–$T_{\rm eff}$ relation, which requires the surface gravity as input. In the colour–$T_{\rm eff}$ relation, we assumed the spectroscopically determined [Fe/H] $= -1.1$ and $[\alpha/\mathrm{Fe}] = 0.4$, see Marino et al. (2008). We assumed an uncertainty on each $T_{\rm eff}$ of 100 K. We note that, for the seven stars in common with the analysis by Marino et al. (2008), the spectroscopic and photometric $T_{\rm eff}$ agree well within the uncertainties.

For internal consistency, the distance modulus was derived by combining the radii of eclipsing binaries presented in Kaluzny et al. (2013) with the temperatures from Casagrande & VandenBerg (2014), giving $(m - M)_0 = 11.20 \pm 0.10$. We then estimated stellar luminosities using this distance together with the apparent magnitudes and BCs.

Table 1. Properties of the stars with detected solar-like oscillations. V_{dr} is the V-band magnitude from the data set described in D'Antona et al. (2009), corrected for differential reddening using the method described in Milone et al. (2012). T_{eff} is calculated from corrected $B - V$ colour and Casagrande & VandenBerg (2014), the assumed uncertainty on T_{eff} is 100 K (see main text for details).

ID	RA (deg)	Dec. (deg)	2MASS ID	V	V_{dr}	T_{eff} (K)	$\Delta\nu$ (μHz)	ν_{max} (μHz)	Noise (ppm^2 μHz^{-1})
S1	245.850 089	−26.500 147	16232402-2630005	12.777	12.786	4585	1.83 ± 0.02	11.1 ± 0.4	84
S2	245.884 870	−26.439 039	16233236-2626205	13.062	13.021	4715	2.55 ± 0.04	17.2 ± 0.7	211
S3	245.911 908	−26.428 539	16233885-2625427	13.071	13.071	4710	2.62 ± 0.04	17.7 ± 0.7	535
S4	245.820 426	−26.496 641	16231690-2629479	13.096	13.121	4715	2.64 ± 0.02	18.5 ± 0.7	188
S5	245.929 534	−26.468 725	16234308-2628074	13.539	13.583	4847	4.14 ± 0.02	32.5 ± 1.3	387
S6	245.949 526	−26.496 729	16234788-2629482	13.577	13.665	4842	4.30 ± 0.02	32.9 ± 1.3	202
S7	245.841 473	−26.508 892	16232195-2630320	13.645	13.668	4805	4.30 ± 0.02	34.3 ± 1.4	172
S8	245.985 479	−26.424 564	16235651-2625284	13.226	13.411	5672	5.67 ± 0.05	42.1 ± 1.7	192

Table 2. Average mass of stars on the RGB estimated using different observational constraints and scaling relations [equations (1) to (4)]. N is the number of stars included in the average. The masses reported in the last four rows were obtained introducing a correction to the $\Delta\nu$ scaling as described in Section 3.1. The mass of the RHB star (S8) is reported in the last column.

Eq.	$\overline{M_{RGB}}$	$\overline{\sigma_M}$	$\sigma_{\overline{M}}$	N	M_{RHB}
(1)	0.99	0.05	0.02	7	0.79 ± 0.10
(2)	0.78	0.09	0.01	7	0.53 ± 0.12
(3)	0.84	0.06	0.01	7	0.61 ± 0.08
(4)	0.94	0.04	0.02	7	0.73 ± 0.07
			$\Delta\nu_{CORR}$		
(1)	0.84	0.04	0.02	7	0.86 ± 0.11
(2)	0.84	0.09	0.01	7	0.51 ± 0.12
(3)	0.84	0.06	0.01	7	0.61 ± 0.08
(4)	0.84	0.03	0.02	7	0.78 ± 0.08

For each set of masses from equations (1)–(4), formal uncertainties on the individual masses were used to compute a weighted average mass of RGB stars ($\overline{M_{RGB}}$). The uncertainties in these averages were estimated from the weighted scatter in the masses ($\sigma_{\overline{M}}$). To assess how well the formal fitting uncertainties reflected the scatter in the data, we also report in Table 2 the weighted mean uncertainty estimated from the formal uncertainties on the masses ($\overline{\sigma_M}$, see Miglio et al. 2012 for details). In some cases [equations (2) and (3)], the observed scatter is significantly lower than expected from the formal uncertainties, which may indicate an overestimation of the observational uncertainties [e.g. on T_{eff} which have a significant systematic component and a high-power dependence in equations (2) and (3)].

A source of possible systematic bias for masses determined using the average or global asteroseismic parameters are known departures from the classic scaling $\Delta\nu \propto \rho^{1/2}$ (see e.g. discussions in White et al. 2011, Miglio et al. 2012, Miglio et al. 2013a, and Belkacem et al. 2013). Suggested corrections to the $\Delta\nu$ scaling are likely to depend (at a level of few per cent) on the stellar structure itself. To estimate a set of corrections, we computed stellar models using the code MESA (Paxton et al. 2011), taking an initial mass $M = 0.85\,M_\odot$ and heavy element abundance $Z = 0.003$ (obtained using the expression in Salaris, Chieffi & Straniero 1993, and the spectroscopically determined metallicity and alpha-enhancement from Marino et al. 2008). A Reimers' mass-loss efficiency parameter of $\eta = 0.2$ was also assumed. For any given model, we defined $\Delta\nu$ to be a Gaussian-weighted average (full width at half-maximum $= 0.66\,\nu_{max}^{0.88}$; see Mosser et al. 2012), centred in ν_{max}, of the large frequency separations of adiabatic radial modes (for details see Miglio et al. 2013a and Rodrigues et al., in preparation). The $\Delta\nu$ values were normalized so that a solar-calibrated model reproduced the average $\Delta\nu$ observed in the Sun.

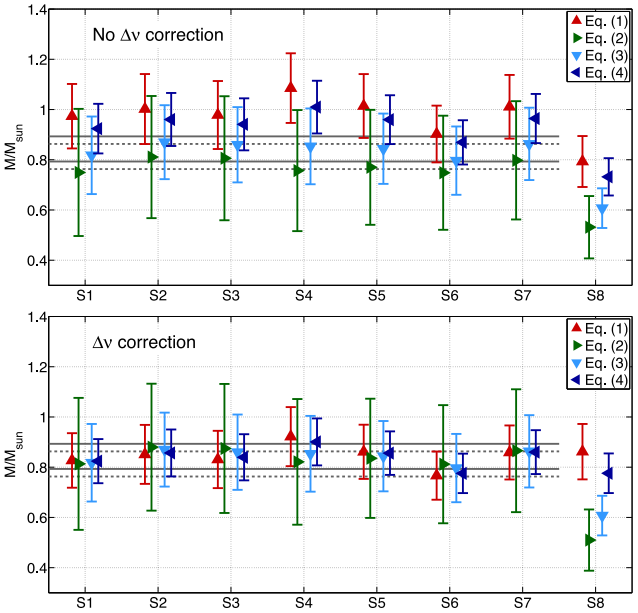

Figure 3. Mass of M4 giants as inferred from equations (1) to (4) with (lower panel) and without (upper panel) applying a model-predicted correction to the $\Delta\nu$ scaling relation. The last star to the right (S8) is an RHB star. The solid and dashed lines denote the 1σ mass interval as determined from isochrone fitting and assuming two values for the initial He mass fraction (see Section 3.1.1 for details).

Our results suggest that the seven RGB stars with detected oscillations are in a ν_{max} range, where the mean density will be underestimated by $\simeq$8 per cent when strict adherence of the classic $\Delta\nu$ scaling is assumed. For the RHB star, the comparison suggests an overestimation of the mean density by $\sim$4 per cent. If we apply these corrections to the mass determinations (see last four rows of Table 2), we end up with a significantly lower scatter in the results (see also Fig. 3) for all RGB stars.

Needless to say, there are other sources of systematic uncertainty that may affect the mass determination (e.g. systematic uncertainties on T_{eff}). A thorough description of the $\Delta\nu$ corrections, their limitations and their dependences on stellar properties, will be presented in Rodrigues et al., in preparation.

Extracting individual mode frequencies from these data is likely to be very challenging. Having estimates of individual frequencies, and not just the average $\Delta\nu$, would allow us to determine the stellar mean density with a much improved precision (see e.g. Huber et al.

2013; Handberg et al., in preparation), and to mitigate the impact of our poor modelling of surface layers (e.g. see Chaplin & Miglio 2013) and of ambiguities in the definition of the average $\Delta\nu$.

3.1.1 Comparison with independent estimates of mass and distance

By fitting to the CMD BaSTI (Pietrinferni et al. 2004) isochrones of the appropriate metallicity and alpha-enhancement, and adopting an initial He mass fraction $Y = 0.25$, we find an age of 13 Gyr and an $M_{\rm ISO,RGB} = 0.84$ M$_\odot$. We adopt a conservative uncertainty of 0.05 M$_\odot$, which takes into account uncertainties on initial chemical composition, age, distance modulus, and reddening. This value for $M_{\rm ISO,RGB}$ is also compatible with the value found by extrapolating with isochrones the mass of the turnoff eclipsing binaries (Kaluzny et al. 2013) to the RGB phase, which gives $M_{\rm EB,RGB} = 0.85$ M$_\odot$.

When the $\Delta\nu$ scaling is taken at face value, $\overline{M_{\rm RGB}}$ determined from the four sets of masses, albeit consistent ($\lesssim$10 per cent) with the expected mass, shows a significant scatter. When introducing a model-based correction to the $\Delta\nu$ scaling relation, the scatter between the various sets of masses is significantly reduced, and the discrepancy with independent mass estimates becomes smaller than the quoted uncertainties on the average mass ($\overline{\sigma_{\rm M}}$) and of the same order or smaller than the weighted scatter in the masses ($\sigma_{\overline{\rm M}}$). A visual comparison between seismic masses and $M_{\rm ISO,RGB}$ is presented in Fig. 3.

The mass of the RHB star is marginally consistent with expectations ($M_{\rm ISO,RHB} \simeq 0.74$ M$_\odot$), and the model-suggested correction increases the scatter between the different mass estimates. Given the uncertainty over mass-loss, and hence on the expected correction to the $\Delta\nu$ scaling, increasing the number of RHB stars with detections will be crucial to quantify any significant bias in the seismic mass estimates.

Several studies have revealed the existence of multiple stellar populations, having different chemical compositions, in globular clusters that have been subjected to a detailed abundance analysis (e.g. see Gratton, Carretta & Bragaglia 2012; Piotto et al. 2015). M4 is no exception, and the presence and properties of two main populations is well documented in the literature (see e.g. Marino et al. 2008; Carretta et al. 2009; Malavolta et al. 2014; Milone et al. 2014). It is widely accepted that the He-poor and He-rich populations in globular clusters are coeval within a few hundreds Myr as predicted by the scenarios proposed to explain the occurrence of these multiple populations (e.g. see Renzini et al. 2015 for a recent review on the proposed scenarios).

The present-day He-rich (Na-rich, O-poor) stars should therefore be less massive than the He-poor (Na-poor, O-rich) stars because the former evolve more quickly. The expected mass difference on the RGB based on the different initial He mass fraction (0.25 versus 0.27; see Nardiello et al. 2015) is inferred to be 0.03 M$_\odot$ (using BaSTI isochrones). A higher He enhancement, as suggested by, for example, Villanova et al. (2012), would imply a higher mass difference (see e.g. Valcarce et al. 2014, for an exhaustive review on recent results). The precision in the average mass determined here is insufficient to detect this difference.

3.2 Radius/distance

Using a combination of seismic constraints and $T_{\rm eff}$, we may also estimate stellar radii:

$$\frac{R}{\mathrm{R}_\odot} \simeq \left(\frac{\nu_{\rm max}}{\nu_{\rm max,\odot}}\right)\left(\frac{\Delta\nu}{\Delta\nu_\odot}\right)^{-2}\left(\frac{T_{\rm eff}}{\mathrm{T}_{\rm eff,\odot}}\right)^{1/2}. \quad (5)$$

Table 3. Mean true distance modulus [DM = $(m - M)_0$] and associated uncertainties, with and without introducing a correction to the $\Delta\nu$ scaling.

$\overline{\rm DM}$	$\sigma_{\overline{\rm DM}}$	$\overline{\sigma_{\rm DM}}$	N	$\Delta\nu_{\rm CORR}$
11.40	0.05	0.02	8	n
11.26	0.05	0.06	8	y

Radii determined from equation (5) agree at the 5 per cent level with independent estimates determined from L and $T_{\rm eff}$.

The above may also be formulated as a comparison of distance moduli. After applying the model-predicted correction to the $\Delta\nu$ scaling, we find an average distance modulus (see Table 3) that is in excellent agreement with the independent determination obtained from constraints on eclipsing binaries (see Section 3.1).

4 SUMMARY AND FUTURE PROSPECTS

We have reported the first detections of solar-like oscillations in giants belonging to a globular cluster. M4 provides what is at present a unique set of targets for testing asteroseismic mass and radius determination in low-metallicity environments. These tests are crucial for the robustness of Galactic archeology studies, which are now making use of solar-like oscillators (see e.g. Miglio et al. 2013b). In the sample of RGB stars analysed in our study, we find no evidence for a significant systematic offset between the seismic mass and radius/distance estimates and independent determinations, provided that a correction to the $\Delta\nu$ scaling relation as suggested by stellar models is introduced. In that case, for RGB stars we find excellent agreement with the expected masses from isochrone fitting, and using a distance modulus derived with independent methods. The offset with respect to independent masses is lower, or comparable with, the uncertainties on the average RGB mass (4–10 per cent, depending on the combination of constraints used).

Extracting clean light curves from these crowded images is challenging, and further complicated by the instrumental drifts of K2. Having demonstrated that it is possible to detect solar-like oscillations in M4, we are now working on producing cleaner light curves for a larger sample of stars. A systematic analysis of asteroseismic detections in a larger sample of M4 giants will allow more stringent tests of the mass determination and, by implication, systematic corrections to the asteroseismic $\Delta\nu$ scaling relation.

The detection of solar-like oscillations potentially opens the door to the more ambitious goal of using seismology to probe multiple populations in old globular clusters. Based on results in the literature (Marino et al. 2008; Carretta et al. 2009), six of the M4 stars with detected oscillations belong to the second (Na-rich, O-poor) population, while the RHB star and S2 are likely to be first generation (Na-poor, O-rich) stars. Again, an increase in the number of stars with detections of solar-like oscillations may allow us to detect mass differences between multiple populations, although the systematic uncertainties described in Section 3 will need to be borne in mind.

Looking to the future, neither the upcoming NASA *TESS* Mission (Ricker et al. 2014) nor the ESA *PLATO* Mission (Rauer et al. 2014) are optimized for the study of densely populated stellar clusters. A space mission dedicated to the detection and study of oscillations in globular clusters should be considered. Long-duration observations, like the multiyear observations provided by the nominal *Kepler* mission, would give the frequency resolution needed to extract individual frequencies of many modes. This would not only improve the determination of global properties (see Section 3.1) but

also give us access to seismic proxies of the internal structures of the stars (i.e. the near-core structure, internal rotation, and information on the envelope He abundance). The limitations imposed by the shorter duration campaigns of K2 mean that extracting individual frequencies of red giants from the existing M4 data will be much more challenging.

ACKNOWLEDGEMENTS

Funding for this Discovery mission is provided by NASA's Science Mission Directorate. The authors wish to thank the entire *Kepler* and K2 team, without whom these results would not be possible. AM, WJC, GRD, YPE, TC, CJ, and JSK acknowledge the support of the UK Science and Technology Facilities Council (STFC). Funding for the Stellar Astrophysics Centre is provided by The Danish National Research Foundation (Grant agreement no.: DNRF106). The research is supported by the ASTERISK project (ASTERoseismic Investigations with SONG and Kepler) funded by the European Research Council (Grant agreement no.: 267864). MNL acknowledges the support of The Danish Council for Independent Research – Natural Science (Grant DFF-4181-00415), and the European Community's Seventh Framework Programme (FP7/2007-2013) under grant agreement no. 312844 (SPACEINN). APM and AFM acknowledge support by the Australian Research Council through Discovery Early Career Researcher Awards DE150101816 and DE160100851. LRB, LM and VN acknowledge PRIN-INAF 2012 funding under the project entitled: 'The M4 Core Project with Hubble Space Telescope'. LM acknowledges the financial support from the European Union Seventh Framework Programme (FP7/2007-2013) under Grant agreement number 313014 (ETAEARTH).

REFERENCES

Baglin A. et al., 2006, 36th COSPAR Scientific Assembly, #3749
Belkacem K., Samadi R., Mosser B., Goupil M.-J., Ludwig H.-G., 2013, in Shibahashi H., Lynas-Gray A. E., eds, ASP Conf. Ser. Vol. 479, Progress in Physics of the Sun and Stars: A New Era in Helio- and Asteroseismology. Astron. Soc. Pac., San Francisco, p. 61
Brogaard K., Sandquist E., Jessen-Hansen J., Grundahl F., Frandsen S., 2015, Ap&SS, 39, 51
Carretta E., Bragaglia A., Gratton R., Lucatello S., 2009, A&A, 505, 139
Casagrande L., VandenBerg D. A., 2014, MNRAS, 444, 392
Chaplin W. J., Miglio A., 2013, ARA&A, 51, 353
Chaplin W. J. et al., 2015, PASP, 127, 1038
D'Antona F., Stetson P. B., Ventura P., Milone A. P., Piotto G., Caloi V., 2009, MNRAS, 399, L151
Frandsen S. et al., 2007, A&A, 475, 991
Gratton R. G., Carretta E., Bragaglia A., 2012, A&AR, 20, 50
Handberg R., Lund M. N., 2014, MNRAS, 445, 2698
Hekker S. et al., 2010, MNRAS, 402, 2049
Hekker S. et al., 2012, A&A, 544, A90
Hendricks B., Stetson P. B., VandenBerg D. A., Dall'Ora M., 2012, AJ, 144, 25
Howell S. B. et al., 2014, PASP, 126, 398
Huber D. et al., 2013, ApJ, 767, 127
Kallinger T. et al., 2014, A&A, 570, A41
Kaluzny J. et al., 2013, AJ, 145, 43
Koch D. G. et al., 2010, ApJ, 713, L79
Lund M. N., Handberg R., Davies G. R., Chaplin W. J., Jones C. D., 2015, ApJ, 806, 30
Malavolta L., Sneden C., Piotto G., Milone A. P., Bedin L. R., Nascimbeni V., 2014, AJ, 147, 25
Marino A. F., Villanova S., Piotto G., Milone A. P., Momany Y., Bedin L. R., Medling A. M., 2008, A&A, 490, 625
Marino A. F., Villanova S., Milone A. P., Piotto G., Lind K., Geisler D., Stetson P. B., 2011, ApJ, 730, L16
Miglio A. et al., 2012, MNRAS, 419, 2077
Miglio A. et al., 2013a, in EPJ Web Conf., 43, 3004
Miglio A. et al., 2013b, MNRAS, 429, 423
Milone A. P. et al., 2012, A&A, 540, A16
Milone A. P. et al., 2014, MNRAS, 439, 1588
Mosser B., Appourchaux T., 2009, A&A, 508, 877
Mosser B. et al., 2011, A&A, 525, L9
Mosser B. et al., 2012, A&A, 537, A30
Mosser B. et al., 2013, A&A, 559, A137
Nardiello D., Milone A. P., Piotto G., Marino A. F., Bellini A., Cassisi S., 2015, A&A, 573, A70
Paxton B., Bildsten L., Dotter A., Herwig F., Lesaffre P., Timmes F., 2011, ApJS, 192, 3
Pietrinferni A., Cassisi S., Salaris M., Castelli F., 2004, ApJ, 612, 168
Piotto G. et al., 2015, AJ, 149, 91
Rauer H. et al., 2014, Exp. Astron., 38, 249
Renzini A. et al., 2015, MNRAS, 454, 4197
Ricker G. R. et al., 2014, in Oschmann J. M., Jr, Clampin M., Fazio G. G., MacEwen H. A., eds, Proc. SPIE Conf. Ser. Vol. 9143, Space Telescopes and Instrumentation 2014: Optical, Infrared, and Millimeter Wave. SPIE, Bellingham, p. 20
Salaris M., Chieffi A., Straniero O., 1993, ApJ, 414, 580
Stello D., Gilliland R. L., 2009, ApJ, 700, 949
Stello D. et al., 2015, ApJ, 809, L3
Valcarce A. A. R., Catelan M., Alonso-García J., Cortés C., De Medeiros J. R., 2014, ApJ, 782, 85
Vanderburg A., Johnson J. A., 2014, PASP, 126, 948
Villanova S., Geisler D., Piotto G., Gratton R. G., 2012, ApJ, 748, 62
White T. R., Bedding T. R., Stello D., Christensen-Dalsgaard J., Huber D., Kjeldsen H., 2011, ApJ, 743, 161

This paper has been typeset from a TEX/LATEX file prepared by the author.